Local variation in the shape of superimposed bed forms as a function of local bathymetry

M.A.F. Knaapen
HR Wallingford, Wallingford, UK

The introduction of multi-beam swath systems gives impressively detailed and accurate information on the sea bed bathymetry. So far however, approaches are missing to extract the vat amounts of information on the morphology from the data. The data contain vital knowledge on bed forms in the field that have not been analysed to their full potential. This paper presents an analysis technique, that determines orientation, wavelength, height and the asymmetry between crest and trough as well as between lee and stoss side of any rhythmic bed form. This approach distillates this shape information for every individual bed form in the measurement domain. Examples given on the application of the approach to data sets of tidal sandbanks, sand waves and mega-ripples results in statistical information on the characteristics of these bed forms. Three findings show the power of the approach, leading to knowledge that is difficult to retrieve in any other way. 1) The height of the tidal sandbanks correlates with depth, such that the depth over the highest point of the crests is uniform at about 21m. 2) The height of mega-ripples superimposed on sand waves depends on the bed level variation of the sand waves. The ratio of the height on the sand wave crest and trough equals the ratio of the sediment transport on the crest and trough of the sand waves. 3) The wavelength of sand waves show a rhythmic variation with a wavelength of 1.5 km. In individual profiles these relationship are disguised by random variations, but the large number of data points generated using our approach does disclose this information.

1 INTRODUCTION

The introduction of state-of-the-art measurement techniques has lead to large amounts of accurate bathymetric data. Multi-beam swath systems measure bands of seabed on high spatial resolutions. Knaapen et al. (2005) for example achieve a 0.3m resolution on 25 meters depth. When combined met high precision Ernstsen (2006), this gives impressive detailed and accurate bed levels of the sea bed. So far however, these data are not analyzed to their full potential. Approaches are missing to extract the essential information from the data. This gap in knowledge is very obvious in the analysis of bed forms on the sea bed. Often, they are used only to visualize the subject, or analyzed by hand to derive information that could be gathered with single-beam echo sounders.

Recently, progress has been made. Knaapen et al (2005), Knaapen (2005) and Ernstsen (2006a), all determine bed form migration for multiple crests, relating it to the height and wavelength of the bed forms. The approach proposed by Knaapen (2005) allows this analysis to be applied to very large amounts of bed form crests. This paper presents an improved and extended analysis technique that gives an improved height estimate and gives additional information on the shape and orientation of the bed forms.

The sandy beds of shallow seas are covered by a wide range of rhythmic bed forms. These patterns range from the very small ripples that can be found at the beach near the water line, to the largest tidal sand banks that are well known because of their risk for ships. In between, a range of wavy patterns exist, which all vary in wavelength, height and orientation (Table 1). We will apply the proposed data analysis technique to mega-ripples, sand waves and sand banks. This approach leads to the amounts of information on the bed patterns that can be used to determine statistical information on the properties of the bed forms in the field. The interpretation of these statistics results in some challenging findings.

Section 1 describes the different steps in the approach to analyze bed forms. Section 2 presents the data to which the analysis approach is being applied. The results are given in section 3 and discussed in section 4. Finally, section 5 summarises the conclusion from the research.

2 BED FORM ANALYSIS MULTI-BEAM DATA

Knaapen (2005) and Knaapen et al (2005) were the first publications describing the analysis of large sets of multi-beam bathymetric data to determine the characteristics of offshore bed forms: sand waves and mega-ripples, respectively. For this purpose an automated approach is used. This approach leads to the amounts of information on the bed forms that are necessary to test models on. Here, we extend their approach to include a measure for the sand volume within the profile, which also is a measure for the crest-trough asymmetry, and crest orientation. Additionally, the height estimate of Knaapen (2005) is replace by a more accurate estimate.

2.1 *Orientation angle*

The first step in the analysis of the bed forms is to determine their orientation, here defined as the direction perpendicular to the crest line. The orientation is determined based on the gradients in the bathymetry, following the approach of Bazen and Gerez (2002). They determined orientation of ridges on gray-scale fingerprints, but the same principles are valid for bed forms in bathymetric data. This approach is based on the principle that in regular rhythmic patters the steepest gradient is perpendicular to the direction of the crests. The orientation angle between the gradient vector and the x-coordinate is defined as:

$$\varphi = \tfrac{1}{2}\,\mathrm{atan}\left(\frac{2\,G_{xy}}{G_{xx} - G_{yy}}\right) + \varphi_c \qquad (1)$$

in which G_{ij} is the product of the gradient in direction i and the gradient in direction j:

$$G_{xx} = \left(\frac{\partial z}{\partial x}\right)^2$$

$$G_{yy} = \left(\frac{\partial z}{\partial y}\right)^2 \qquad (1)$$

$$G_{xy} = \frac{\partial z}{\partial x}\frac{\partial z}{\partial y}$$

and φ_c is a correction to make correct for the fact that areas on opposite sites of the crests have opposing gradient vectors:

$$\varphi_c = \pi \;\forall G_{x^2} - G_{y^2} < 0 \;\&\; G_{x^2} - G_{y^2} \geq 0$$

$$\varphi_c = -\pi \;\forall G_{x^2} - G_{y^2} < 0 \;\&\; G_{x^2} - G_{y^2} < 0$$

$$\varphi_c = 0 \;\forall G_{x^2} - G_{y^2} \geq 0$$

If one applies this algorithm to the matrix containing the sea bed bathymetry, it produces an array of local estimates of the orientation of the smallest bed form. Therefore, one has to smooth the bathymetric data removing all bed forms smaller than the bed form of interest. A window size that is about half the wavelength of the targeted bed form gives reliable and robust results.
Now that the orientation of the bed forms is know, one can analyze the other shape characteristics along crest-normal profiles.

2.2 *Determining the crest and trough positions*

Based on the orientation, the bathymetric data is interpolated to a regular orthogonal grid with the main axis in the direction of the bed form orientation. Taking the profiles in the direction of the bed form orientation, which is normal to the crests, the crest and trough positions in bed forms are identified following an improved approach to the one proposed by Knaapen (2005).
In that approach, the bathymetry is smoothed using weighted averaging in which the weight reduces linearly with distance (Bartlett window). The size of this window is depends on the typical wavelength of the targeted bed form. It should be less considerably less than this wavelength but larger than the typical size smaller bed forms. A window size that is about half the wavelength of the targeted bed form gives reliable and robust results.
The crests and troughs are than defined as the highest and lowest points in the profiles of the smoothed profiles. The weighted averaging leads to an underestimation of the crest position, especially in case of sharp crested sand waves. In the new approach, we fit a forth order polynomial through the original measurements that are in the neighborhood of the extreme points in the smoothed profile. Once the crest and trough positions are known, they are analyzed to retrieve information on the wavelength, height and asymmetry. Although the definition of these characteristics is straightforward, to calculation them from the observed crests and troughs one has to make a few assumptions.

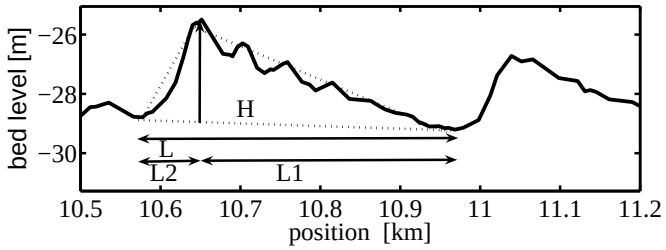

Figure 1. Definition of the height H, length L and asymmetry of the bed forms as function of the crest and trough levels (After Knaapen, 2005). The dotted triangle defines the triangular surface created to calculate the relative volume of the bed form.

2.2.1 *Wavelength*

The distance between the trough positions on both sides of the crest (x_1, x_2) determines the length of the bed form:

$$L = | x_2 - x_1 | \cos(\alpha)$$

With α being the angle between the mean crest orientation and the direction of the profiles.

2.2.2 *Height*

The height is defined as the difference between the crest levels z_{crest} and the trough levels (z_1,z_2).

$$H = z_{crest} - \frac{z_1 L_2 + z_2 L_1}{L}$$

The height of the pattern is here defined as the height of the envelope resulting from a linear interpolation of the crest en trough levels (see figure 1). This results in heights that are equal to the difference between a crest level and the mean level of the neighboring troughs weighed by the distance between those troughs and the crest.

2.2.3 *Lee-stoss asymmetry*

The lee-stoss asymmetry is defined as the difference of the distance between the trough north of the crest and the distance between the crest and the trough south of the crest divided by the wavelength:

$$A = \frac{L_2 - L_1}{L}$$

Following this definition, a perfect symmetric wave has a asymmetry value A=0.5.

2.2.4 *Volume*

The relative volume is defined as the area of the bed form above the line through both neighboring trough positions divided by the volume of a triangle with the same length and height:

$$V = \frac{\int_{x_1}^{x_2} z - \frac{(z_2 - z_1)dx}{2}}{(x_2 - x_1)\left(z_{crest} - \frac{z_2 - z_1}{2} \right)}$$

in which z is the local bed level. This measure for relative volume gives a value of 0.5 for any sand wave without crest-trough asymmetry and has limits of 0 and 1 for asymmetric waves with infinite narrow crests and troughs respectively. A sand wave with a high and narrow crest, will give a relative volume between 0 and 0.5.

2.3 *Research area and bathymetric data*

The bed form analysis will be performed on a part of the Dutch sand banks in the North Sea. Figure 2 shows the local bathymetry. Three data sets are processed to analyze the sandbanks in this area and superimposed sand waves and mega-ripples in subsets of this area.

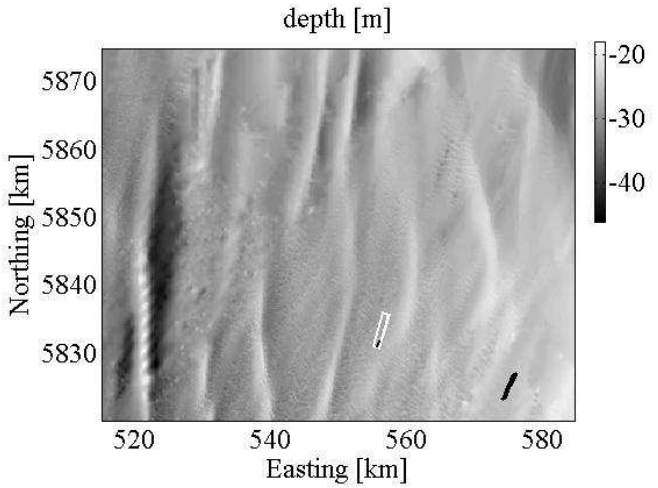

Figure 2. Bathymetry of the research area in the Southern Bight of the North Sea. The bathymetry clearly shows the Dutch Banks, of which the Brown Bank can be recognized in the east. Less visible are the sand waves, with crests about orthogonal to the tidal sand bank crests. The tidal sandbanks will be analyzed for the bathymetry in the whole area, the sand waves (white rectangle) and mega-ripples (black spot within white rectangle) for subsets of this area, that have been measured with higher resolution. Northing and easting are in UTM ED50 projection. The tidal ellipse is shown in lower right corner.

2.3.1 *Sandbanks*

The general bathymetry of the Dutch banks is available in an equidistant matrix with a resolution of 200m. The bathymetry is a mosaic of data collected through time. This will have introduced some errors related to morphodynamic changes. However, given the rate of bathymetric change, the positional errors are assumed to be in the order of about 10m and the vertical error in the order of about 25cm. Both are small compared to the sizes of the sandbanks.

The tide is fairly unidirectional, with a maximum depth averaged flow velocity of 0.81ms^{-1}. The sediments consist of medium fine sands with a mean diameter of 0.225mm in the north to 0.275mm in the south of the area McCave (1971).

2.3.2 *Sand waves*

Within the general bathymetry, an area of 5x1km^2 has been surveyed within a single multi-beam swath survey (figure 3). The center of this area is located at 556274m Easting and 5833391m Northing. The longer axis of the area makes a 16 degrees angle to the North. This area is on average about 28m deep and is covered by sand waves superimposed on the slope of a tidal sandbank. Locally the sediments is

well sorted D_{60}/D_{10}=1.5 and a median grain size of 0.275mm with some sorting effects between crest and trough Passchier and Kleinhans (2005). The depth averaged tidal velocity is about 0.7ms^{-1} at a tidal range of 0.6m.

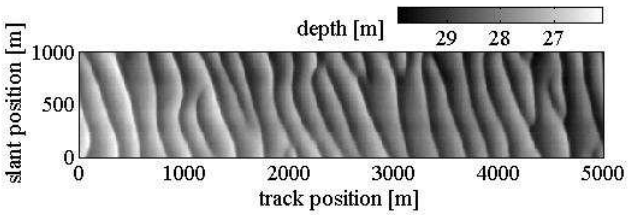

Figure 3. Sand wave field superimposed on the Dutch banks. Position is in orthogonal coordinates relative to the most southern point of the rectangle.

The data with a resolution of about $2.5m$ in both directions was interpolated linearly to an equidistant grid with the same resolution in both directions. The orientation of this grid is such that one axis is approximately parallel to the sand wave crests and the other one orthogonal to them.

For this survey, the positioning system has an error with a 2.5m standard deviation Knaapen et al (2005). The depth measurements still have a standard deviation of about 20cm. However, the major part of this error is related to the tidal correction of the depth. Since the measurement time is relatively short this part of the error is about the same throughout the whole domain and will not influence the analysis performed here. The remaining standard deviation in the vertical is about 5 to 10cm. This is sufficiently small for the approach to give reliable estimates.

2.3.3 *Mega-ripples*

A subset of the sand wave area, with a surface area of 500x75m^2 has been surveyed within a single multi-beam swath track. The direction of this swath has a 26^o angle clockwise with the North, which is about perpendicular to the crest of the mega-ripples (figure 4). The center of this area is located at 556274m Easting and 5833391 Northing. This area is on average about 28m deep and is covered by mega-ripples superimposed on sand waves on the slope of a tidal sandbank.

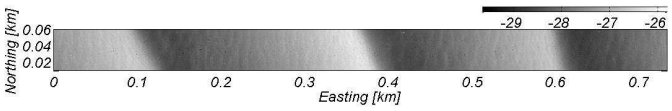

Figure 4. Mega-ripple field superimposed on the sand waves. Position is in orthogonal coordinates relative to the most southern point of the rectangle.

The multi-beam echo soundings have a resolution of about 0.35m, which we interpolated to a equidistant grid with the same resolution. For this survey, taken in 2002, the positioning system has similar errors as the sand wave survey of section 2.3.2. The effective error in the vertical is 5 to 10cm. The error of the positioning error is about 2.5m. However, about 2m is related to the correction relative to the base station which is constant throughout the domain. No information was available about the standard deviation of the remaining error. This error is almost purely random, which makes it possible to analyze bed forms that have amplitude with the same magnitude as the measurement noise.

3 RESULTS

The approach to analyze bathymetric data on bed forms is applied to the three data sets. First, the height predictions with the polynomial approach are compared to the predictions by the approach of Knaapen (2005) (section 3.1). After that we will show some examples of bed patterns analysis applied to sandbanks (section 3.2), sand waves (section 3.3) and mega-ripples (section 3.4).

3.1 *Height estimates*

The proposed use of a fourth order polynomial to estimate the bed level of the crests and troughs removes the noise from smaller bed patterns without the underestimation of the height resulting from the weighted averaging. Figure 5 shows the differences between the raw data and the smoothed data for the polynomial estimate and the window averaging estimate for the measured sand waves.

The estimates of the window averaging show a larger error that still depends on depth and thus on the sand wave height. Consequently, the sand wave height is being underestimated. The differences between the raw data and the polynomial fit are much smaller and are independent of depth. The remaining difference has the same magnitude as half the height of the superimposed smaller bed forms.

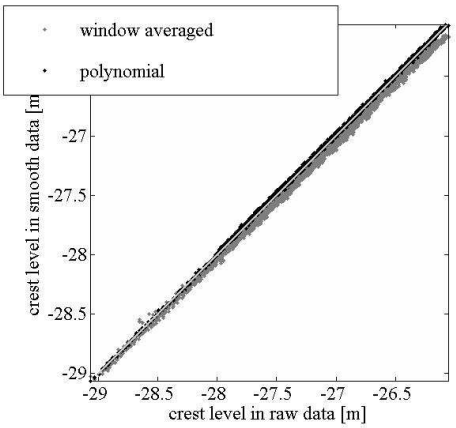

Figure 5. The differences between the raw crest levels and the values after window smoothing (black) and the polynomial fit (gray) for the and waves.

3.2 *Sandbanks*

This data set is analyzed in the east-west direction, since the sandbank crests are almost parallel to the north-axis. Figure 6 shows the crest of the sandbanks in the research area. Additionally, the color of the dots denotes the height of the sandbank at that point.

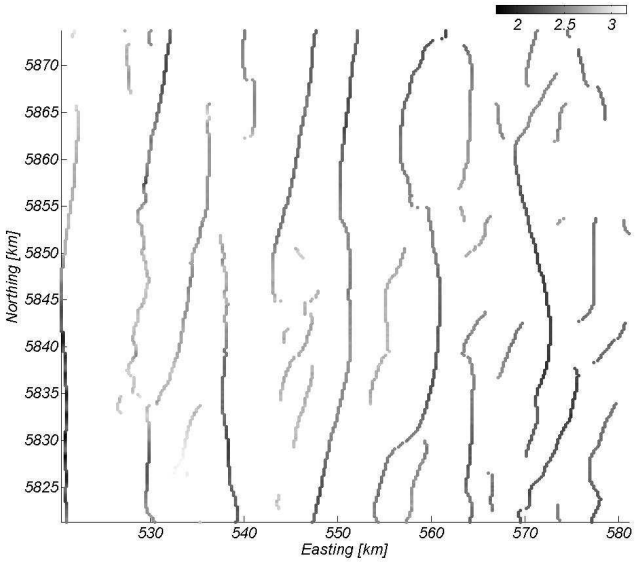

Figure 6. The crests of the tidal sand banks in the research area with the height estimates indicated by the color. Coordinates in UTM kilometers.

The sandbank height shows an increase going east. This trend is confirmed when looking at the maximum crest level as function of the easting position. The increase in crest height compensates the increase in mean depth completely, resulting in an almost constant value of the minimum navigation depth (Figure 7) of about 21m. No other characteristic shows any structural variation within the domain.

The number of crests in the area is limited. A statistical analysis of the characteristics for this data set is not very reliable.

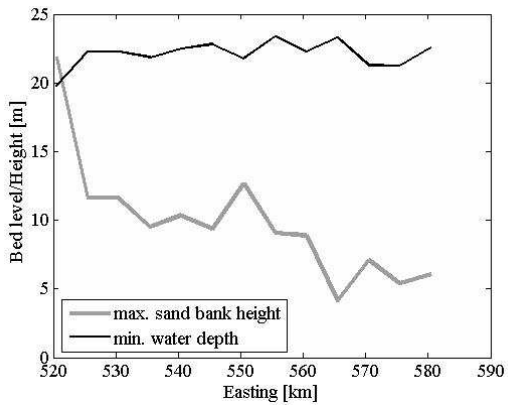

Figure 7. Sandbank height and minimum water depth as function of easting. Easting in UTM kilometers.

3.3 *Sand waves*

The sand wave orientation is approximately 30 degrees clockwise with respect to the North. The crest trough analysis shows that the sand waves are very regular, with only a few bifurcations (figure 8).

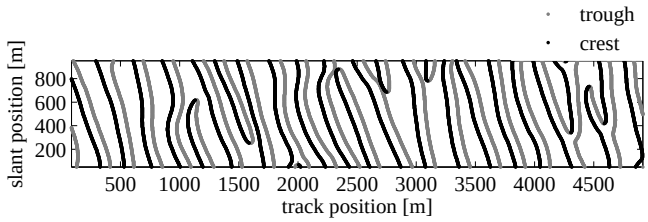

Figure 8. The crests (black) and troughs (gray) of sand waves in the research area. The coordinates are given in meters and the principal tidal direction is from left to right.

This observation is confirmed and quantified by the statistics and the probability density functions (figure 9). The pdf's of all characteristics show a symmetric bell-shape curve suggesting a Gaussian distribution. The wavelength has a mean value of 201m, with a standards deviation of 44m. The height has a mean of 1.6m, with a 0.4m standard deviation.

The crests and trough lines in figure 8 are pairwise close together, which shows asymmetry. The histogram of the asymmetry in figure 9 confirms this observation, showing a narrow peak at 0.2. On average the south-western slopes are 50\% longer than the North-eastern slopes.

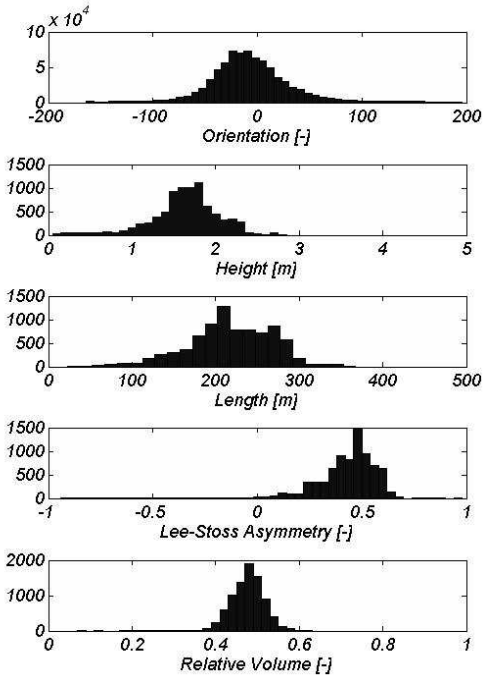

Figure 9. Histograms of the orientation, the height, the wavelength the asymmetry and the relative volume of the sand waves.

There is little asymmetry between the crests and troughs, with a relative volume of 0.48; the sand waves have an almost perfect saw-tooth shape.

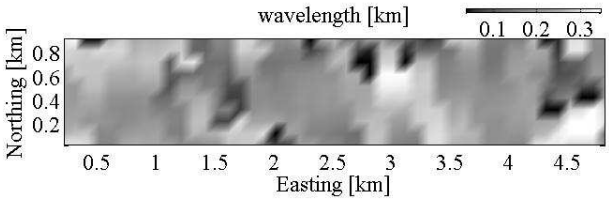

Figure 10. The variation of the sand wave length over the measurement area.

From the pdf's one can deduct that the variation in the sand waves is very limited. Still there is some variation. The second axis in figure 9 shows a peak with a wide shoulder for higher wavelengths. Figure 10 shows the wavelength over the area after linear interpolation to a 100x100m^2 grid. In this figure one can see an alternating pattern of areas in which the wavelength is 200m and areas in which both larger and smaller wavelengths, related to the bifurcations, coexist. Apparently, the deviations from the mean wavelength occur grouped in bands with a wavelength of about 1.5km.

3.4 *Mega-ripples*

The minima-maxima analysis applied to the mega-ripple data results in the crests and troughs positions shown in figure 11. The approach detects no mega-ripples on the steeper slopes of the underlying sand waves. However, close inspection of the topography faintly shows some low mega-ripples in this location.

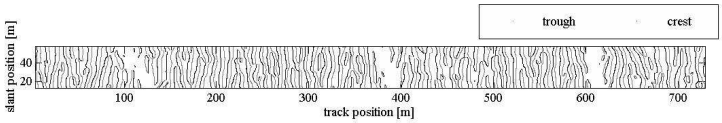

Figure 11. The crests and troughs of mega-ripples in the research area. Coordinates in meters.

Figure 12 gives the pdf's of the orientation, length, height, asymmetry and relative volume of the mega-ripples. The mean wavelength is about 8.7m, with a standard deviation of 2.1m. The mean height is about 30cm, but occasionally mega-ripples are found that are much higher. On average the mega-ripples are symmetrical, with the majority having only very small asymmetry.

The height of the mega-ripples shows a correlation with the position on the sand waves. Figure 13 shows the mega-ripple height as function of the undisturbed water depth, e.g. the local water depth has been corrected for the disturbance by the mega-ripples. Although the random variations exceed the trend, the mega-ripples on the troughs are on average 10 cm higher than the ones in the troughs.

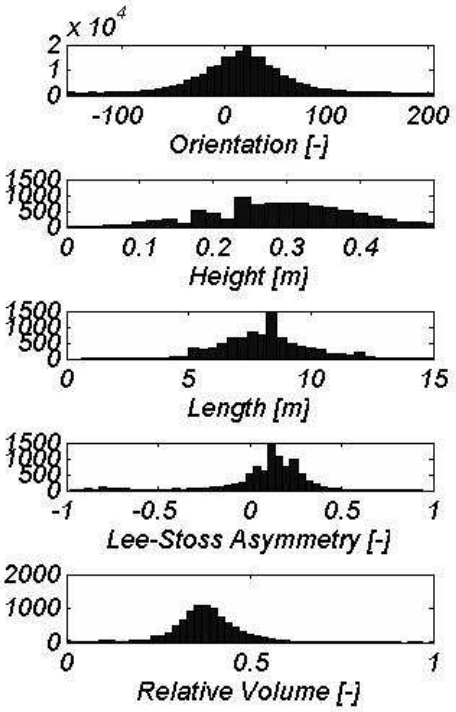

Figure 12. Histograms of the orientation, the height, the wavelength the asymmetry and the relative volume of the mega-ripples.

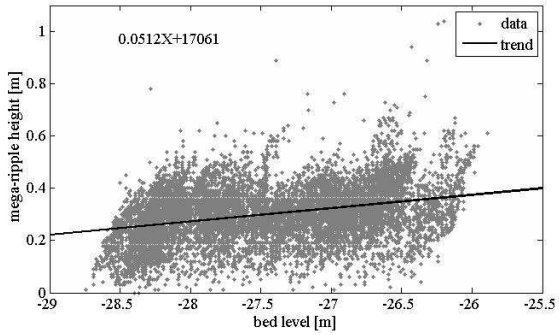

Figure 13. The mega-ripple height as function of undisturbed water depth (i.e. without mega-ripples)

4 DISCUSSION

The proposed data analysis approach captures almost all bed waves we have analyzed. It did not detect the low amplitude mega-ripples on the steep slope of the underlying sand waves. The sand wave slope and the mega-ripple height are such, that the up-slope mega-ripple trough is only marginally lower than the crest. As a result one or two mega-ripples are missed on the lee-side of each sand wave. This absence of some data hardly influences the statistics which are based on a far larger number of mega-ripples. The biggest effect is a distortion of the characteristics of the first mega-ripples next to the steep slope. Their length, asymmetry and relative volume are distorted. In the pdf (figure 12) this shows up as long tails. Note that the tail of the wavelength is outside the limits of the axis.

In principle, the algorithms presented here to determine height, length and asymmetries works independent of the orientation of the profile relative to the crest orientation. One only needs to correct the wavelength by multiplication of the length along the profile with the cosine of the angle between profile direction and bed form orientation. However, if the angle gets to large and the sinuosity of the crest lines is large, the crest detection will start missing the crest points, whose orientation is close to the orientation of the profile. Therefore, it is advised to work with profiles that are about perpendicular to the mean orientation of the bed pattern.

The proposed analysis gives accurate estimates of the characteristics of bed forms with statistical descriptions, which cannot be achieved with current approaches. Passchier and Kleinhans 2005 for example only give the ranges of the height and length of mega-ripples, whereas we present more detailed information based on the same bathymetric information. The large number of data points makes it possible to reliably detect relationships that are relatively weak compared to the noise. The constant water depth over the sand bank crests would be difficult to determine from an individual profile, as the maximum crest heights of different sandbanks don't line up along a single line. Similarly, the wavelength variation of the sand waves can only be detected in the 2D distribution of the wavelengths over space. The relationship between mega-ripple height and depth does show up from individual profiles. However, only the repeated result from several profiles increases the reliability of the found relationship.

With exception of the Brown Bank, the sandbanks in this area are much lower than the better known sandbanks in the North Sea, such as the Flemish Banks or the Norfolk Banks, reaching no more than 25% to 50% of the maximum water depth. The location of the research area is fairly close to the amphidromic point resulting in lower tidal currents; the driving mechanism is less strong. This suggests that the Brown Bank, which is much higher, is (partly) relic.

The variation in the depth-to-height ratio of the sandbanks, even ignoring Brown bank, contrasts with the findings of theoretical work, which assumes that the sandbank height is a fairly constant percentage of the maximal water depth (Idier and Astruc, 2002). The marginal variations in tidal strength or sediment characteristics

McCave (1971) cannot explain the variations in the height-to-depth ratio. This height variation of the sandbanks results in an almost constant water depth over the highest point of the crest, about 21m. This might be explained by the assumptions of Huthnance (1982) and Roos (2004) that the tide is driving the generation of the sandbanks whereas the wave forcing is limiting the crest level to a constant level. Along the research area, the wave climate is uniform leading to uniform water depths above the rests.

The height of mega-ripples also correlates with the local water depth. The mega-ripple heights at the sand wave crests are (0.35-0.22)/0.35=24.8% higher than in the troughs. A straight forward analysis shows that the difference in the potential sediment transport between crests and the troughs of the sand waves has the same ratio. As the principal tidal current is almost perpendicular to the sand wave crests, the flow velocities at the crests will be larger than the velocities in the troughs. Mass conservation gives that the flow velocity is about 28.5/26.5=1.075% higher over the crests than over the troughs (see for example Hulscher, 1996).

Sandbank related sediment is assumed to be a function of the cubed flow velocity. So the magnitude of the sediment transport will be 1.075^3-1=24.4% higher on the crests.

No height variations could be discovered in the sand waves, but this might just be because the bed level variation over the measurement domain is to small. The sand waves do show a variation in wavelength. It is impossible to explain these rhythmic variations based on the measurements only. However, the 1.5km wavelength of these variation is similar to the wavelength of the long bed waves described by Knaapen (2001).

The orientation of the bed forms is linked to the direction of the tidal current. Hulscher (1996) explains why the crests of tidal sandbanks have a small counterclockwise rotation with respect to the principal axis of the tidal ellipse and that the crests of sand waves are at small angles to that principal axis. Similarly, the crests of mega-ripples are generally perpendicular to the direction of the flow. The observations here agree well with these assumptions for the tidal sandbanks 68^o. The angle between the principal axis of the modeled tide and the crests of the sand waves -34^o and mega-ripples -9^o is slightly higher than expected (17^o and 0^o respectively). This difference is provoked by the disturbances of the tide due to the presence of the tidal sandbanks.

The tide has been calculated on a grid with a spacing that is too large to include the tidal sandbanks. These flat bed calculations are perfect to estimate the angle of the sandbanks, but introduce errors if looking at superimposed smaller bed forms.

5 CONCLUSIONS

In this paper, a automated variation on a classical approach is followed to analyze bed forms from multi-beam bathymetric surveys. After the orientation is determined, the data the crest and troughs are detected objectively along profiles that are perpendicular to the sand wave crests. The detection is reliable, robust and easily implemented.

This approach results in large data sets on the both the position and levels of the crests and the troughs. These data sets are then easily transformed into information on the characteristics of the bed waves: wavelength, height and the asymmetry (crest vs. trough and lee vs. stoss side).

The resulting data have been analysed to evaluate the characteristics of three bed forms occurring in a part of the North Sea where they occur superimposed on each other: sandbanks, sand waves and mega-ripples.

It is shown, that the height of the sandbanks and the mega-ripples correlates with depth. Whereas the maximum water depth increases from 25m in the East to 40m in the West, the minimum water depth over the crests is constant at about 20m. The mega-ripples on the sand wave crests are larger than the ones in the sand wave troughs. For sandwaves such a relationship could not be determined.

The difference is of the same order as the difference in potential sediment transport between the crests and roughs. The wavelength of the observed sand waves shows an unexplained rhythmic variation with a 1.5km wavelength.

6 ACKNOWLEDGEMENT

Major parts of the work presented here has been done at the University of Twente, the Netherlands, financially supported by the Delft Cluster Programme of the Dutch government, by the European Union within the framework of the HUMOR project (EVK3-CT-2000-00037) and by the Technology Foundation STW, applied science division of NWO and the technology program of the Ministry of Economic Affairs (project number TWO.5805). The data presented here has been made available by Dr. Passchier of TNO/NITG in the Netherlands and Mr. Bicknese of the North Sea Directorate of the Netherlands Ministry of transport, Public Works and Water Management.

7 REFERENCES

Bazen, A.M. and Gerez, S.H. 2002. Systematic methods for the computation of the directional fields and singular points of fingerprints. *IEEE transactions on pattern analysis and machine intelligence*, 24 (7): 905-919, July 2002.

Dodd, n, Blondeaux, P. Calvete, D. De Swart, H.E. Falques, A. Hulscher, S.J.M.H. Rozynski, G. and Vittori, G. 2003. The use of stability methods for understanding the morphodynamical behaviour of coastal systems. *Journal of Coastal Research*, 19 (4), 2003.

Ernstsen, V.B., Noormets, R. Hebbeln, D. Bartholoma, A. and Flemming, B.W. 2006. Precision of high-resolution multibeam echo sounding coupled with high-accuracy positioning in a shallow water coastal environment. *Geo-Marine Letters*, 26 (3): 141-149.

Ernstsen, V.B. Noormets, R. Hebbeln, D., Winter, C. D. Bartholoma, A. Flemming, B.W. and Bartholdy, J. 2006a. Quantification of dune dynamics during a tidal cycle in an inlet channel of the Danish Wadden Sea. *Geo-Marine Letters*, 26 (3): 151-163.

Hulscher. S.J.MM.H. 1996. Tidal-induced large-scale regular bed form patterns in a three-dimensional shallow water model. *Journal of Geophysical Research*, 101 (C9): 20,727-20,744.

Huthnance, J. 1982. On the formation of sand banks of finite extent. *Estuarine Coastal Shelf Sciences*, 14: 277-299.

Idier, I. and Astruc, D. 2002. Analytical and numerical modeling of sandbanks dynamics. *Journal of Geophysical Research*, 108 (C3): 3060-3074.

Knaapen, M.A.F. Sand wave migration predictor based on shape information. *Journal of Geophysical Research*, 110.

Knaapen, M.A.F. Hulscher, S.J.M.H. De Vriend, H.J. and Stolk, A. 2001. A new type of bedwaves. *Geophysical Research Letters*, 28 (7): 1323-1326.

Knaapen, M.A.F. Van Berge Henegouw, C.N. and Hu, Y.Y. Quantifying bedform migration using multi-beam sonar. *Geo-Marine Letters*, 25 (5): 306 – 314.

McCave, N. 1971. Sand waves in the North Sea off the coast of Holland. *Marine Geology*, 10: 199-225.

Passchier S. and Kleinhans, M.G. Observations of sand waves, megaripples, and hummocks in the Dutch coastal area and their relation to currents and combined flow conditions. *Journal of Geophysical Research*, 110 (F4): F04S15.

Reineck, H.E. Singh, I.B. Wunderlich, F. 1971. Einteilung rippen und anderer mariner sandkörper. *Senckenbergiana maritima*, 3: 93-101.

Roos, P.C. Hulscher, S.J.M.H. van Damme, R. and Knaapen, M.A.F. 2004. The cross-sectional shape of tidal sandbanks: Modeling and observations. *Journal of Geophysical Research*, 109 (F02003).